Gas Phase Reactions of HONO with NO_2, O_3, and HCl: Ab Initio and TST Study

Xin Lu,† J. Park, and M. C. Lin*

Department of Chemistry, Emory University, Cherry L. Emerson Center of Scientific Computation, Emory University, Atlanta, Georgia 30322

Received: April 26, 2000; In Final Form: July 20, 2000

Gas-phase reactions of HONO with species of atmospheric interest, NO_2, O_3, and HCl, have been investigated by means of ab initio molecular-orbital and transition-state theory calculations. For the HONO + NO_2 reaction, the most favorable pathway is found to be the abstraction of OH in HONO by NO_2, leading to the formation of HNO_3 and NO products. The activation energies computed at the G2M (RCC,MP2) level of theory for the abstraction from *trans*- and *cis*-HONO are predicted to be 31.6 and 33.4 kcal/mol, respectively. At 300 K, the calculated rate constant is smaller than 1.2×10^{-14} cm^3 mol^{-1} s^{-1}. For the HONO + O_3 reaction, the barrier height for the production of $HNO_3 + O_2$ is predicted to be 15.0 kcal/mol with the rate constant at 300 K, 5.7×10^{-2} cm^3 mol^{-1} s^{-1}. For the *trans*- and *cis*-HONO + HCl → H_2O + ClNO reactions, our G2M calculations predict the corresponding barrier heights of 12.9 and 14.4 kcal/mol with predicted rate constants, 1.3×10^2 and 0.13×10^2 cm^3 mol^{-1} s^{-1} at 300 K. The results of our theoretical modeling indicate that the three gas-phase reactions are too slow to be significant under the stratospheric and tropospheric conditions.

Introduction

Nitrous acid (HONO) is a key reactive intermediate in the combustion of many nitramine propellants;[1−4] it is also a potential source of hydroxyl radical in the troposphere through photolytic reactions.[5] On account of its relevancy in combustion and atmospheric chemistry, there has been considerable interest in studying the chemical properties and the reactions of nitrous acid, experimentally and theoretically. Besides some recent theoretical studies, which focus on the properties of nitrous acid as well as its van der Waals complexes,[6−10] a series of ab initio molecular-orbital (MO) and transition-state theory (TST) calculations of HONO reactions in the gas phase have been performed in our laboratory. The reactions that have been theoretically studied are the oxidation of HNO by NO_2 to produce HONO and NO,[11] the bimolecular self-reaction of HONO,[12] the reduction of HONO by HNO and NH_3,[13] the oxidation of HONO by NO_2 and O_3, and the reaction of HONO with HCl. In the present paper, we report our theoretical results for the latter three gas-phase reactions of HONO with NO_2, O_3, and HCl.

Although these title reactions, as pointed out above, are directly relevant to both atmospheric chemistry[14−16] and the combustion of propellants, there are very few experimental studies regarding these processes. The tunable diode laser study of the HNO_3 + NO → HNO_2 + NO_2 reaction performed by Streit et al.[14] appears to be the only experimental work related to the kinetics of the HONO + NO_2 reaction. They also investigated the HONO + O_3 → HNO_3 + O_2 reaction. They estimated the upper limits of the rate constants at room temperature for the reactions with NO_2 and O_3 to be 60 and 2.7 $\times 10^5$ cm^3 mol^{-1} s^{-1}, respectively.[14] A similar estimation was made for the latter reaction by Kaiser et al.[15] However, the inevitable presence of H_2O, NO, and NO_2 in the reactor, which may induce interfering side reactions,[14,15] decreases the reliability of those kinetic measurements. For the HONO + HCl → ClNO + H_2O reaction, if it occurred readily, the ClNO product could potentially undergo photodissociation to produce the ozone-destructive chlorine atom.[17] Recent experiments[17,18] reveal that this reaction can occur both homogeneously and heterogeneously. The experimentally estimated upper limit of the rate constant for the homogeneous gas-phase reaction is ∼1.1 $\times 10^5$ cm^3 mol^{-1} s^{-1} at 297 K.[18]

The small experimental values of the rate constants for these reactions suggest that they may not contribute significantly in the chemistry of stratosphere and troposphere. To elucidate the mechanisms of these reactions and to make a reliable assessment of their roles in the atmospheric chemistry, we have carried out a detailed ab initio MO and TST study; the theoretical results are presented herein.

Computational Details

The geometries of the reactants, products, intermediates, and transition states of the three title reactions have been fully optimized by using the hybrid density functional B3LYP method (Becke's three-parameter nonlocal exchange functional[19−21] with the correlation functional of Lee, Yang, and Parr[22]) using the 6-311G(d,p) basis set.[23] Vibrational frequencies employed to characterize stationary points and make zero-point energy (ZPE) corrections have also been calculated at this level of theory and used for the subsequent transition-state theory (TST) calculations of reaction rate constants. All the stationary points have been positively identified for local minima (with the number of imaginary frequencies, NIMAG = 0) and transition states (with NIMAG = 1). To confirm that the transition states connect between designated intermediates, we have performed intrinsic reaction coordinate (IRC) calculations[24] at the B3LYP/6-311G-(d,p) level. All the energies quoted and discussed in the present article include ZPE corrections.

To obtain more reliable energies, we have carried out

* To whom correspondence should be addressed. E-mail address: chemmcl@emory.edu.

† Permanent address: State Key Laboratory for Physical Chemistry of Solid Surfaces and Department of Chemistry, Xiamen University, Xiamen 361005, P. R. China.

10.1021/jp001610o CCC: $19.00
Published on Web 08/25/2000

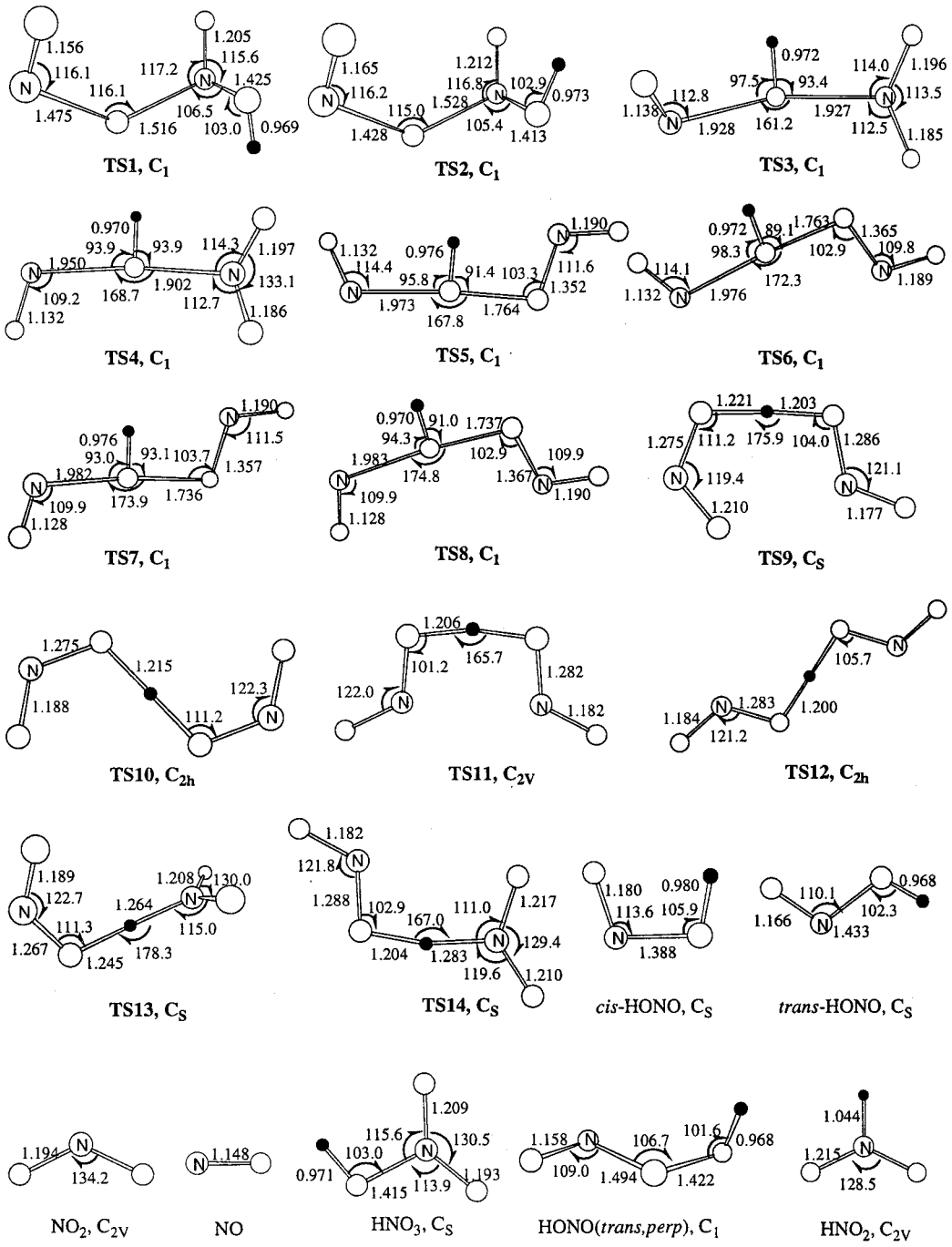

Figure 1. B3LYP/6-311G(d,p) optimized structures (bond lengths in Å, bond angles in degrees) of the reactants, transition states, and products of the HONO + NO_2 reaction.

restricted closed-shell and open-shell coupled cluster RCCSD-(T)/6-311G(d,p)[25] as well as G2M(RCC,MP2)[26] calculations. The G2M(RCC,MP2) method is a modification of the Gaussian-2 (G2) approach;[27] it uses B3LYP/6-311G(d,p) optimized geometries and substitutes the QCISD(T)/6-311G(d,p)[28] calculation of the original G2 scheme with the RCCSD(T)/6-311G-(d,p) calculation. The total energy in G2M(RCC,MP2) is obtained as follows:[26]

$$E[\text{G2M(RCC,MP2)} = E[(\text{RCCSD(T)/6-311G(d,p)}] + \Delta E(+3\text{df,2p}) + \Delta E(\text{HLC}) + \text{ZPE}$$

where

$$\Delta E(+3\text{df,2p}) = E[\text{MP2/6-311+G(3df,2p)}] - E[\text{MP2/6-311G(d,p)}]$$

and the empirical "higher level correction"(HLC) in mhartree

$$\Delta E(\text{HLC}) = -5.25n_\beta - 0.19n_\alpha$$

where n_α and n_β are the numbers of α and β valence electrons, respectively. All the ab initio calculations were performed using the GAUSSIAN94[29] and MOLPRO96[30] programs.

Results and Discussions

A. HONO + NO_2 Reaction. For the HONO + NO_2 reaction in the gas phase, there are several possible, distinct reaction pathways that lead to the formation of different sets of products,

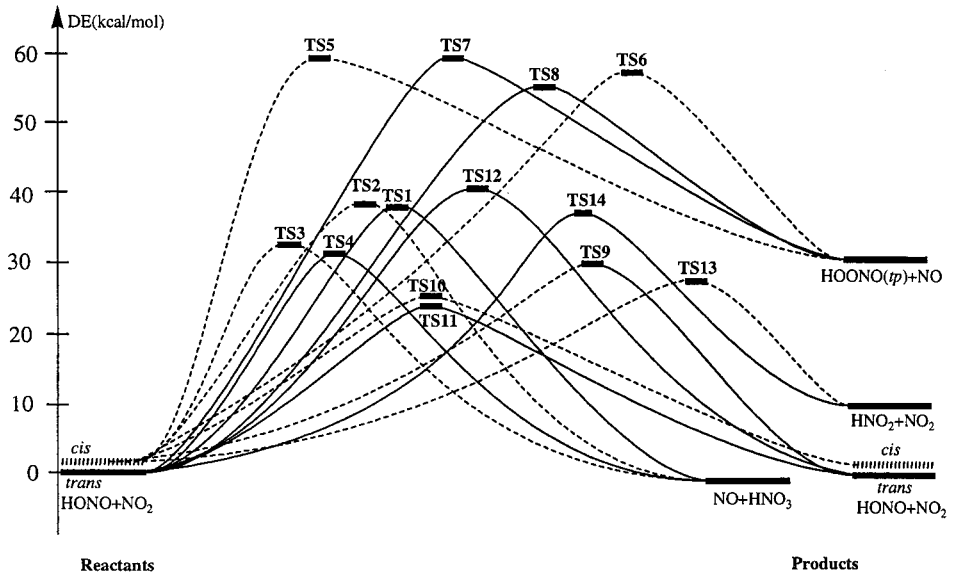

Figure 2. Energy diagram for the potential energy surface of the HONO + NO_2 reaction calculated in the framework of the G2M(RCC,MP2)// B3LYP/6-311G(d,p) approach. Solid lines connect the *trans*-HONO related channels, and the dotted lines connect the *cis*-HONO related channels.

TABLE 1: Energetics[a] of the Reactants, Products, Intermediates, and Transition States of the NO_2 + HONO Reaction at Different Levels of Theory

	ZPE[b]	B3LYP/6-311G(d,p)	CCSD(T)/6-311G(d,p)	G2M(RCC,MP2)
trans-HONO + NO_2	18.3	−410.89449[c]	−409.97393[c]	−410.29142[c]
cis-HONO + NO_2	18.3	−410.89487[c]	−409.97449[c]	−410.29071[c]
		−0.2	−0.4	+0.4
TS1	18.9	32.2	37.9	38.0
TS2	18.9	32.7	38.1	38.5
TS3	17.9	23.9	33.6	33.8
TS4	18.2	21.6	31.9	31.6
TS5	16.9	50.4	55.6	59.3
TS6	16.6	49.4	54.7	58.1
TS7	17.1	47.4	56.0	59.3
TS8	16.9	46.9	50.6	54.6
TS9	16.8	13.8	29.9	29.3
TS10	16.4	9.7	24.6	23.5
TS11	17.2	12.3	25.5	21.7
TS12	16.6	17.1	40.7	38.8
TS13	16.6	12.8	25.7	26.0
TS14	16.9	20.5	35.4	35.9
NO + HOONO(*tp*)	17.3	34.7	29.3	30.8
NO_2 + HNO_2	19.3	7.2	10.1	8.7
NO + HNO_3	19.4	1.4	−3.2	−0.6 (−0.1)[d]

[a] Relative energy with respect to NO_2 + *trans*-HONO. [b] Zero-point energy corrections (kcal/mol), calculated at the B3LYP/6-311G(d,p) level. [c] Total energies given in hartrees. [d] Experimental value from ref 31 is given in parentheses.

i.e.,

O abstraction by HONO:

$$\textit{cis}\text{- or }\textit{trans}\text{-HONO} + \text{ON}\mathbf{O} \rightarrow \text{HNO}_3 + \mathbf{N}\text{O} \quad (1)$$

OH abstraction by NO_2:

$$\textit{cis}\text{- or }\textit{trans}\text{-HONO} + \mathbf{N}\text{O}_2 \rightarrow \text{NO} + \text{HN}\mathbf{O}_3 \quad (2)$$

$$\rightarrow \text{NO} + \text{HOON}\mathbf{O} \quad (3)$$

H abstraction by NO_2:

$$\textit{cis}\text{- or }\textit{trans}\text{-HONO} + \mathbf{N}\text{O}_2 \rightarrow \text{NO}_2 + \text{HN}\mathbf{O}_2 \quad (4)$$

$$\rightarrow \text{NO}_2 + \textit{cis}\text{-HON}\mathbf{O} \text{ (or } \textit{trans}\text{-HON}\mathbf{O}\text{)} \quad (5)$$

The optimized geometries of the reactants, products, and transition states for the above pathways are shown in Figure 1. The potential energy curves connecting the reactants, transition states, and the corresponding products are depicted in Figure 2. The relative energies of all the species obtained at different levels of theory are listed in Table 1 and their vibrational frequencies and moments of inertia in Table 2. All the results presented in this section, including the energy profiles presented in Figure 2, are based on the G2M energies unless otherwise specified.

O Abstraction by HONO. First we consider reaction pathway 1 proceeding by the abstraction of the oxygen atom from NO_2 by HONO. Two transition states, **TS1** and **TS2**, which derive, respectively, from *trans*-HONO + NO_2 and *cis*-HONO + NO_2, have been located in the PES. The corresponding activation energies are predicted to be of the same value, 38 kcal/mol. The calculated exothermicities for the formation of HNO_3 + NO from the reaction of the *trans*- and *cis*-HONO isomers are 0.6 and 1.0 kcal/mol, respectively, in reasonable accord with the experimental values, 0.1 and 0.6 kcal/mol.[31]

OH Abstraction by NO_2. As alluded above, the abstraction

TABLE 2: Molecular and Transition-State Parameters of the Reactants, Products, and Transition States of the HONO + NO_2 Reaction, Used for the TST Calculations of the Rate Constants[a]

species	I_i (amu)	frequencies (cm^{-1})
trans-HONO	19.2, 143.9, 163.1	591, 618, 834, 1298, 1793, 3776
cis-HONO	21.3, 136.0, 157.3	638, 719, 892, 1338, 1721, 3584
NO_2	7.5, 138.3, 145.8	767, 1399, 1706
TS1	285.2, 578.9, 609.5	294*i*, 101, 177, 246, 343, 491, 537, 550, 653, 849, 915, 1307, 1518, 1798, 3760
TS2	285.6, 572.2, 584.7	365*i*, 111, 179, 255, 314, 491, 535, 554, 673, 879, 928, 1345, 1496, 1756, 3703
TS3	175.4, 1300.4, 1440.3	617*i*, 45, 60, 111, 197, 292, 357, 363, 490, 778, 1044, 1370, 1774, 1924, 3739
TS4	174.6, 1265.7, 1438.1	615*i*, 47, 86, 111, 205, 318, 347, 375, 487, 781, 1061, 1372, 1766, 1971, 3771
TS5	109.6, 1517.2, 1619.8	607*i*, 44, 60, 108, 215, 241, 281, 347, 461, 673, 875, 1193, 1663, 1978, 3663
TS6	70.5, 1631.4, 1697.2	604*i*, 19, 57, 100, 184, 193, 278, 338, 455, 643, 843, 1150, 1664, 1975,3744
TS7	61.0, 1625.2, 1686.2	599*i*, 42, 98, 125, 199, 220, 345, 353, 450, 673, 890, 1202, 1670, 2012, 3693
TS8	141.6, 1397.9, 1539.5	592*i*, 39, 78, 101, 209, 260, 274, 298, 466, 650, 864, 1156, 1670, 2008, 3780,
TS9	214.6, 808.7, 1023.3	1688*i*, 72, 155, 163, 255, 298, 498, 779, 835, 1222, 1275, 1302, 1457, 1659, 1760
TS10	171.7, 1051.6, 1223.2	1581*i*, 8, 101, 129, 213, 346, 511, 761, 872, 1188, 1200, 1272, 1554, 1636, 1653
TS11	206.0, 950.0, 1156.0	1563*i*, 89, 121, 183, 186, 294, 506, 823, 883, 1193, 1281, 1302, 1649, 1661, 1859
TS12	49.8, 1608.6, 1658.3	1808*i*, 23, 62, 164, 190, 206, 467, 812, 892, 1191, 1276, 1284, 1602, 1671, 1748
TS13	261.8, 965.3, 977.5	1672*i*, 48, 82, 121, 333, 385, 420, 803, 852, 1257, 1391, 1400, 1431, 1633, 1656
TS14	163.7, 1090.5, 1254.2	2008, 71, 72, 179, 255, 379, 406, 791, 880, 1144, 1255, 1360, 1603, 1620, 1747
NO	35.2, 35.2	1988
HOONO(*tp*)	33.1, 367.8, 395.1	212, 293, 358, 459, 809, 1015, 1408, 1822, 3751
HNO_2	16.7, 136.8, 153.5	800, 1069, 1408, 1542, 1678, 3145
HNO_3	138.5, 149.8, 288.3	482, 588, 654, 776, 911, 1327, 1359, 1778, 3737

[a] Calculated at the B3LYP/6-311G(d,p) level.

of the OH group from HONO may proceed by NO_2 attack on the O(H) of HONO with either N or O, leading to the formation of HNO_3 or HOONO (peroxynitrous acid), respectively. Reaction 2 has the same exothermicity as reaction 1 because both reactions have common reactants and products. Reaction 3 is predicted to be endothermic, as HOONO is known to be a high energy isomer of HNO_3.[32,33]

For reaction 2, two transition states, **TS3** and **TS4**, have been found (see Figure 1). **TS3** connecting *cis*-HONO + NO_2 with the HNO_3 + NO products has an energy barrier of 33.4 kcal/mol, while **TS4** connecting *trans*-HONO + NO_2 with the same products has a slightly lower energy barrier, 31.6 kcal/mol. It is thus clear that for the production of HNO_3, the two channels (via **TS3** and **TS4**) of reaction 2 are preferable over the two channels via **TS1** and **TS2** in reaction 1, as the latter pathways require higher energy barriers (~38 kcal/mol).

For reaction 3 producing HOONO + NO, four transition states, namely, **TS5**, **TS6**, **TS7**, and **TS8**, have been located in the PES. Both **TS5** and **TS6** are formed by *cis*-HONO + NO_2, and **TS7** and **TS8** are formed by *trans*-HONO + NO_2. IRC calculations reveal that these four TSs all lead to the common products, *trans,perp*-HOONO [see HOONO(*tp*) in Figure 1] plus NO, despite that HOONO itself has three possible conformers, namely, *cis,cis*-HOONO, *cis,perp*-HOONO, and *trans,perp*-HOONO.[32,33] Further isomerization of HOONO into HNO_3 is kinetically prohibitive in the gas phase, as shown by recent ab initio calculations.[33,34] Furthermore, its high endothermicity (30.8 kcal/mol) and activation energy (the lowest barrier height is 54.6 kcal/mol at **TS8**) imply that reaction 3 is practically not important to the HONO + NO_2 reaction.

H Abstraction by NO_2. H abstraction from HONO by NO_2 producing different HONO isomers is indeed a process of NO_2-catalyzed isomerization of HONO. Totally six transition states (**TS9**−**TS14**) have been located for such a catalytic isomerization. **TS9** connects *cis*-HONO + NO_2 with NO_2 + *trans*-HONO. **TS10** connects *cis*-HONO + NO_2 with NO_2 + *cis*-HONO. **TS11** and **TS12** connect *trans*-HONO + NO_2 with NO_2 + *trans*-HONO. **TS13** and **TS14** are the transition states for the *cis*-HONO + NO_2 ⇔ NO_2 + HNO_2 and *trans*-HONO + NO_2 ⇔ NO_2 + HNO_2 reactions, respectively. The activation energies required for these six channels range from 21.6 kcal/mol (**TS11**) to 38.8 kcal/mol (**TS12**). It is obvious that these channels are practically inconsequential to the HONO + NO_2 reaction, insofar as the overall chemistry is concerned.

Rate Constant Calculations by TST. We have shown by ab initio MO calculations that the two OH abstraction processes, *cis*-HONO + NO_2 → **TS3** → HNO_3 + NO and *trans*-HONO + NO_2 → **TS4** → HNO_3 + NO, are energetically more favorable and are potentially key channels for the HONO + NO_2 reaction in the gas phase. TST calculations were carried out to obtain their rate constants, using the reaction barriers and molecular parameters given in Tables 1 and 2. The rate constant expressions obtained by two-parameter fitting for 300−1000 K and three-parameter fitting for the 300−3000 K temperature range are given in Table 3, along with the derived apparent activation energies and the rate constants at 300 K. At 300 K, the calculated rate constants, k_I and k_{II}, for the cis- and trans- reactions are 9.4×10^{-14} and 1.2×10^{-12} cm^3 mol^{-1} s^{-1}, respectively. The two theoretical values are considerably lower than the experimentally estimated upper limit of 60.3 cm^3 mol^{-1} s^{-1}.[15] These results suggest that the oxidation of HONO by NO_2 is too slow to be important in the chemistry of atmosphere. It may be relevant to the combustion of nitramine propellants under high temperature and pressure conditions, however.

B. HONO + O_3 Reaction. The optimized geometries of the reactants, transition states and products of this reaction are presented in Figure 3, and the corresponding energetics are tabulated in Table 4. The potential energy curves connecting the reactants, transition states, and the corresponding products are depicted in Figure 4. The vibrational frequencies and moments of inertia calculated at the B3LYP level are given in Table 5.

Potential Energy Surface. The reaction producing HNO_3 + O_2 ($^3\Sigma_g^-$) is predicted to be exothermic by −44.4 kcal/mol at the G2M level, in reasonable agreement with the experimental value, −47.1 kcal/mol.[31] The initial spin-allowed products of the reaction are HNO_3 + O_2 ($^1\Delta$) according to the result of an IRC test. At the G2M level of theory, the predicted energy difference between the $^1\Delta$ and $^3\Sigma_g^-$ states of O_2 is 25.6 kcal/mol, somewhat higher than the experimental value, 22.6 kcal/mol.[35] Five transition states, **TS1′**−**TS5′** (Figure 3), have been

TABLE 3: Calculated Rate Constants (cm^3 mol^{-1} s^{-1}) and Apparent Activation Energies (kcal/mol) for the HONO + NO_2, HONO + O_3, and HONO + HCl Reactions

	3-param (300∼3000 K)	300 K	2-param (300∼1000 K)	E_a
$HONO + NO_2 \rightarrow HNO_3 + NO$				
NO_2 + *cis*-HONO, k_I	$3.03 \times 10^2\ T^{3.33} \exp(-16427/T)$	9.36×10^{-14}	$1.18 \times 10^{13} \exp(-18171/T)$	36.1
NO_2 + *trans*-HONO, k_{II}	$2.00 \times 10^2\ T^{3.28} \exp(-15445/T)$	1.22×10^{-12}	$5.49 \times 10^{12} \exp(-17165/T)$	34.1
$HONO + O_3 \rightarrow HNO_3 + O_2\ (^1\Delta)$				
O_3 + *trans*-HONO, k_{III}	$0.153\ T^{3.22} \exp(-10839/T)$	3.04×10^{-9}	$2.79 \times 10^9 \exp(-12530/T)$	24.9
O_3 + *cis*-HONO, k_{IV}	$0.707\ T^{3.41} \exp(-6606/T)$	5.73×10^{-2}	$5.07 \times 10^{10} \exp(-8396/T)$	16.7
$HONO + HCl \rightarrow H_2O + ClNO$[a]				
HCl + *trans*-HONO, k_V	$1.05 \times 10^2\ T^{3.02} \exp(-5122/T)$	1.27×10^2	$4.02 \times 10^{11} \exp(-6647/T)$	13.2
HCl + *cis*-HONO, k_{VI}	$0.69 \times 10^2\ T^{3.12} \exp(-5867/T)$	0.13×10^2	$5.55 \times 10^{11} \exp(-7443/T)$	14.8

[a] Eckart tunneling correction was used to compute the rate constants.

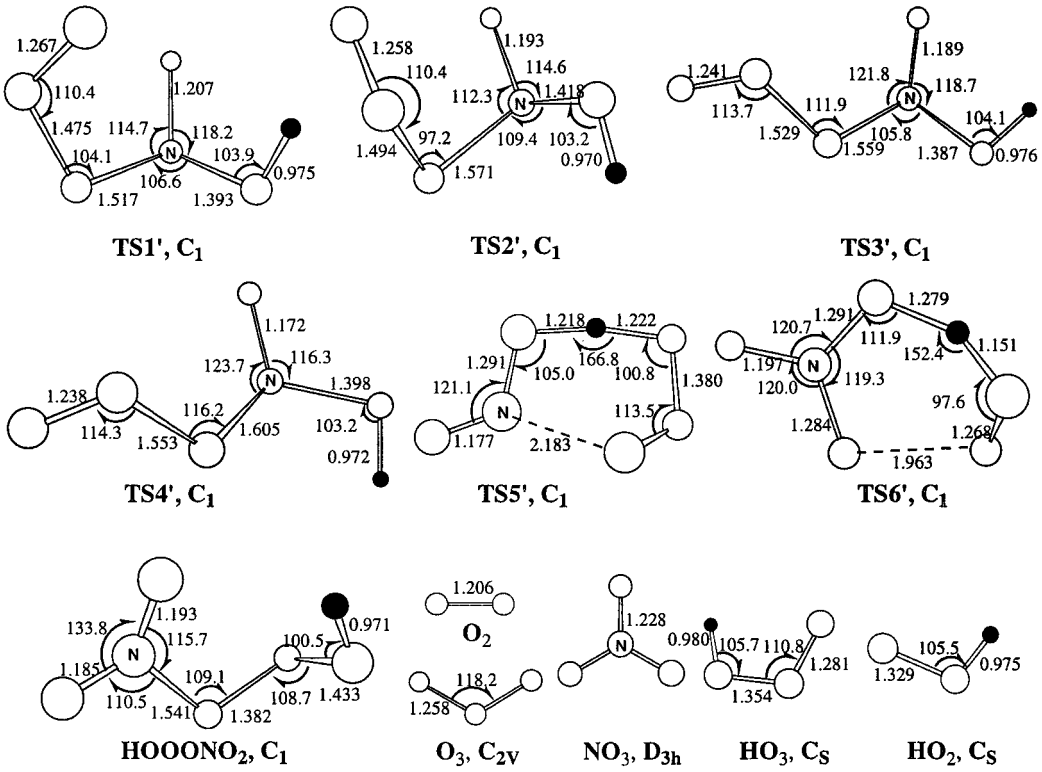

Figure 3. B3LYP/6-311G(d,p) optimized structures (bond lengths in Å, bond angles in degrees) of O_2, O_3, and the transition states of the HONO + O_3 reaction.

located in the PES of the reaction. The transition states, **TS1′** and **TS3′**, derived from *cis*-HONO + O_3, have the barrier heights of 26.1 and 15.0 kcal/mol, whereas **TS2′** and **TS4′** from the *trans*-HONO + O_3 reactants have the values of 23.7 and 26.1 kcal/mol, respectively. Hence, the *cis*-HONO reaction via **TS3′** is most favorable.

We have also found the transition state, **TS5′**, that leads to the formation of $HOOONO_2$. To the best of our knowledge, no experimental observation of this molecule has been reported; its possible existence was first predicted by Li and Iwata in their recent study of the cyclic isomers of HNO_x ($x = 2-6$).[36] $HOOONO_2$ was found to be most stable among the four HNO_5 conformers studied.[36] Our G2M calculations predict that the formation of the species is exothermic by 16.7 kcal/mol with a barrier of 23.9 kcal/mol. Theoretically, $HOOONO_2$ may undergo unimolecular decomposition reactions forming $HO_3 + NO_2$ and $HO_2 + NO_3$ with the predicted dissociation energies of 17.6 and 29.4 kcal/mol, respectively. In addition, it may also decompose via **TS6′**, producing $HNO_3 + O_2$ with a barrier of 21.9 kcal/mol (see Figure 3).

Rate Constant Calculations. The rate constants for the reaction of O_3 with *trans*- and *cis*-HONO have been calculated with TST. The expressions for the two rate constants obtained by 2-parameter fitting for 300−1000 K and 3-parameter fitting

TABLE 4: Energetics[a] of the Reactants, Products, Intermediates, and Transition States of the HONO + O_3 Reaction at Different Levels of Theory

	ZPE[b]	B3LYP/ 6-311G(d,p)	CCSD(T)/ 6-311G(d,p)	G2M (RCC,MP2)
trans-HONO + O_3	17.3	−431.23256[c]	−430.28920[c]	−410.62971[c]
cis-HONO + O_3	17.3	−431.23294[c]	−430.28976[c]	−430.62900[c]
TS1′	18.4	25.6	31.4	26.5
TS2′	18.4	27.4	32.8	23.7
TS3′	21.7	38.3	18.2	15.4
TS4′	17.8	32.0	31.6	26.1
TS5′	16.2	9.5	24.4	23.9
TS6′	17.7	−9.6	5.1	5.2
$HOOONO_2$	20.3	−25.9	−14.9	−16.7
$NO_2 + HO_3$	16.6	−16.0	−0.9	0.9
$NO_3 + HO_2$	15.6	−12.0	6.9	12.7
$HNO_3 + O_2\ (^1\Delta_g)$	18.9	−21.9	−21.4	−18.8
$HNO_3 + O_2\ (^3\Sigma_g^-)$	18.9	−60.9	−52.1	−44.4 (−47.1)[d]

[a] Relative energy with respect to *trans*-HONO + O_3. [b] Zero-point energy corrections (kcal/mol), calculated at the B3LYP/6-311G(d,p) level. [c] Total energies given in hartrees. [d] Experimental value from ref 31 is given in parentheses.

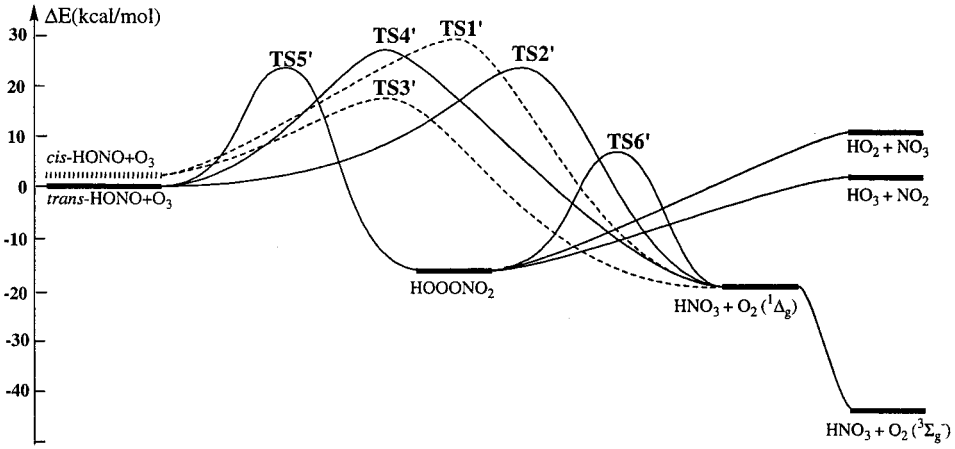

Figure 4. Energy diagram for the potential energy surface of the HONO + O_3 reaction calculated in the framework of the G2M(RCC,MP2)//B3LYP/6-311G(d,p) approach. Solid lines connect the *trans*-HONO related channels, and the dotted lines connect the *cis*-HONO related channels.

TABLE 5: Molecular and Transition-State Parameters of the Reactants, Products, and Transition States of the HONO + O_3 Reaction, Used for the TST Calculations of the Rate Constants[a]

species	I_i (amu)	frequencies (cm^{-1})
trans-HONO	see Table 2	see Table 2
cis-HONO	see Table 2	see Table 2
O_3	15.9, 133.0, 148.9	747, 1191, 1249
TS1′	257.3, 546.6, 626.4	610*i*, 134, 225, 307, 385, 472, 613, 618, 712, 767, 911, 1168, 1372, 1492, 3668
TS2′	284.0, 519.1, 610.2	647*i*, 166, 211, 332, 377, 491, 582, 605, 678, 735, 867, 1204, 1326, 1554, 3757
TS3′	174.1, 874.5, 1005.9	826*i*, 71, 121, 176, 281, 404, 501, 611, 633, 751, 893, 1299, 1364, 1614, 3645
TS4′	182.7, 907.6, 1043.1	837*i*, 35, 101, 167, 270, 440, 490, 601, 629, 716, 880, 1316, 1345, 1712, 3729
TS5′	227.4, 748.0, 935.9	1546*i*, 76, 163, 195, 299, 456, 510, 701, 832, 972, 1173, 1211, 1240, 1694, 1824
TS6′	189.9, 679.4, 840.1	1063*i*, 102, 223, 336, 416, 557, 709, 777, 791, 1014, 1213, 1327, 1407, 1625, 1887
$HOOONO_2$	205.5, 680.6, 800.7	108, 149, 327, 402, 451, 499, 644, 723, 784, 866, 961, 1361, 1407, 1823, 3715
HO_2	2.9, 53.5, 56.4	1163, 1428, 3610
NO_3	130.3,130.3, 260.6	259(2), 802, 1121(2), 1135
HO_3	26.1, 155.7, 181.8	236, 453, 704, 1234, 1403, 3687
O_2 ($^1\Delta_g$)	41.6, 41.6	1626
O_2 ($^3\Sigma_g^-$)	41.5, 41.5	1641
HNO_3	138.5, 149.8, 288.3	482, 588, 654, 776, 911, 1327, 1359, 1778, 3737

[a] Calculated at the B3LYP/6-311G(d,p) level.

for 300−3000 K are given in Table 3, along with the apparent activation energies and the values at 300 K. For the most favored reaction, *cis*-HONO + O_3, the predicted rate constant, k_{IV}, at 300 K is 5.7×10^{-2} cm^3 mol^{-1} s^{-1}; it is higher by 7 orders of magnitude than that for *trans*-HONO + O_3, $k_{III} = 3.0 \times 10^{-9}$ cm^3 mol^{-1} s^1. The experimentally estimated upper limit at 300 K is 2.7×10^5 cm^3 mol^{-1} s^{-1},[14] which is significantly higher than the predicted values.

C. HONO + HCl Reaction. The optimized geometries of the reactants, transition states, and products of this reaction are presented in Figure 5, and the corresponding energetics are tabulated in Table 6. The potential energy curves connecting the reactants, transition states, and the corresponding products are depicted in Figure 6. The vibrational frequencies and moments of inertia calculated at the B3LYP/6-311G(d,p) level are given in Table 7.

Potential Energy Surface. We have located four transition states, **TS1″** to **TS4″** (see Figure 5), responsible for four distinct reaction pathways. **TS1″** derives from *trans*-HONO + HCl and leads to the formation of H_2O and ClNO products. At the G2M level, the reaction is predicted to be exothermic by 5.5 kcal/mol with a barrier height of 12.9 kcal/mol. IRC calculations, however, located two local minima, **LM1** and **LM2**, along this reaction pathway. **LM1** is a H-bonding complex of the reactants *trans*-HONO + HCl, whereas **LM2** is a H-bonding complex of the products H_2O + ClNO. Both H-bonding complexes have been detected experimentally by matrix isolation infrared spectroscopy and also confirmed by ab initio MO calculations.[37,38] The reaction of *cis*-HONO with HCl via **TS2″** leads to the same products as the *trans*-reaction via **TS1″**. The G2M barrier height and the heat of reaction for the *cis*-channel are 14.4 and −5.9 kcal/mol, respectively. In this channel, a H-bonding complex of *cis*-HONO and HCl, **LM3**, exists as a precursor. As far as the reverse reaction (H_2O + ClNO → HCl + HONO) is concerned, the formation of *trans*-HONO is favored by 1.9 kcal/mol over the formation of the *cis*-isomer.

The third channel, *trans*-HONO + HCl → **LM4** → **TS3″** → **LM5** → HNO_2 + HCl, may be regarded as a HCl-catalyzed isomerization of HONO. A similar process has been found in our study of the NH_3 + *trans*-HONO system.[13] The G2M barrier height for the catalytic isomerization is 18.5 kcal/mol, far lower than that for the direct unimolecular *trans*-HONO → HNO_2 isomerization (55.2 kcal/mol).[13] It should be mentioned that for the NH_3-catalyzed process, our G2M barrier is 21.3 kca/mol.[13] Hence, both acid (HCl) and base (NH_3) facilitate the H-migration and enhance *trans*-HONO → HNO_2 isomerization significantly in the gas phase.

The transition state, **TS4″**, connects two equivalent isomers of **LM6**, a H-bonding complex of HCl + *cis*-HONO, and gives rise to the H-exchange between HCl and *cis*-HONO. This H-exchange reaction, among all the four channels considered, has the lowest activation energy (12.3 kcal/mol at the G2M level), but it does not result in a chemical change. Therefore,

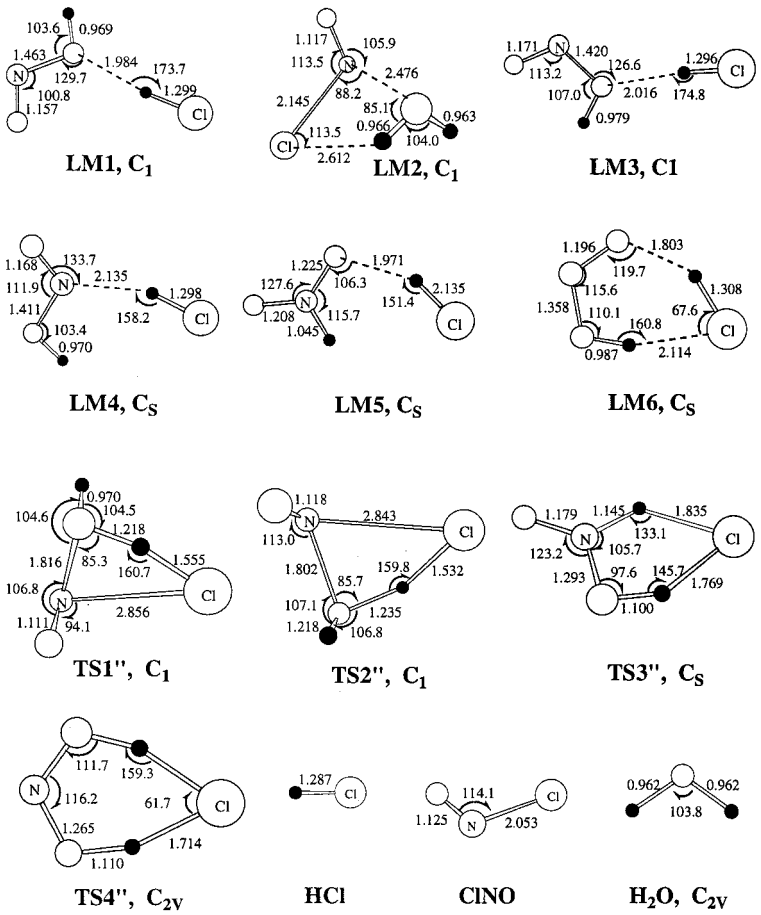

Figure 5. B3LYP/6-311G(d,p) optimized structures (bond lengths in Å, bond angles in degrees) of HCl, ClNO, H_2O, and the transition states of the HONO + HCl reaction.

TABLE 6: Energetics[a] of the Reactants, Products, Intermediates, and Transition States of the HONO + HCl Reaction at Different Levels of Theory

	ZPE[b]	B3LYP/ 6-311G(d,p)	CCSD(T)/ 6-311G(d,p)	G2M (RCC,MP2)
trans-HONO + HCl	16.9	−666.59523[c]	−665.56155[c]	−665.81099[c]
cis-HONO + HCl	16.9	−666.59562[c]	−665.56211[c]	−665.81028[c]
TS1″	16.9	10.3	13.6	12.9
TS2″	16.7	11.2	15.3	14.8
TS3″	18.4	16.6	21.9	18.5
TS4″	17.3	11.7	15.4	12.7
LM1	18.0	−3.8	−5.2	−4.3
LM2	19.4	−6.9	−5.4	−6.4
LM3	17.9	−3.1	−4.7	−3.6
LM4	18.3	0.1	−2.9	−3.6
LM5	19.4	4.0	5.4	3.7
LM6	18.0	−1.7	−3.4	−3.3
HNO_2 + HCl	17.9	7.3	10.1	8.7
ClNO + H_2O	17.5	−2.3	−3.0	−5.5 (−5.0)[d]

[a] Relative energy with respect to *trans*-HONO + HCl. [b] Zero-point energy corrections (kcal/mol), calculated at the B3LYP/6-311G(d,p) level. [c] Total energies given in hartrees. [d] Experimental value (ref 31) is given in parentheses.

in the following TST calculations, we do not take this channel into account.

Rate Constant Calculations. The rate constants for the channels, *trans*-HONO + HCl → **LM1** → **TS1″** → **LM2** → ClNO + H_2O and *cis*-HONO + HCl → **LM3** → **TS2″** → **LM2** → ClNO + H_2O, have been calculated by using the TST with Eckart tunneling corrections.[39] The expressions for the rate constants (k_V and k_{VI}) obtained by 2-parameter fitting in the temperature range 300−1000 K and by 3-parameter fitting in the temperature range 300−3000 K are given in Table 3, along with the derived apparent activation energies and the rate constants at 300 K. Experimentally, an upper limit of the gas-phase HONO + HCl → ClNO + H_2O reaction at 297 K has been reported to be $\sim 1 \times 10^5$ cm^3 mol^{-1} s^{-1},[18] which is higher than our predicted value (1.3×10^2 cm^3 mol^{-1} s^{-1}) by several orders of magnitude.

It is worthwhile to compare this reaction with the analogous process,

$$\mathrm{HONO + HONO \rightarrow H_2O + [N_2O_3] \rightarrow H_2O + NO + NO_2}$$

which has been thoroughly studied in our laboratory recently with the G2M method.[12] The lowest energy path in this reaction involves *cis*- and *trans*-HONO, taking place via a six-membered ring hydrogen-bonded TS with a 13.7 kcal/mol barrier. It is slightly higher than the two lowest barriers for the HCl reaction with HONO, 12.7 kcal/mol via TS4″ and 12.9 kcal/mol via TS1″, despite the large difference in the H−X (X = Cl, ONO) bond strengths. The key factor for the slightly lower barrier for the stronger H−Cl bond may be attributed to the stronger Cl−NO bond (vs the ON−ONO bond) which helps drive the reaction forward. The predicted bimolecular rate constant for the self-reaction of HONO was found to be 4 orders of magnitude lower than the upper limit of Kaiser and Wu,[40] who strongly emphasized the importance of heterogeneous contributions to these types of reactions.

Concluding Remarks

The mechanisms for the gas-phase reactions of HONO with the three species of atmospheric interest, NO_2, O_3, and HCl,

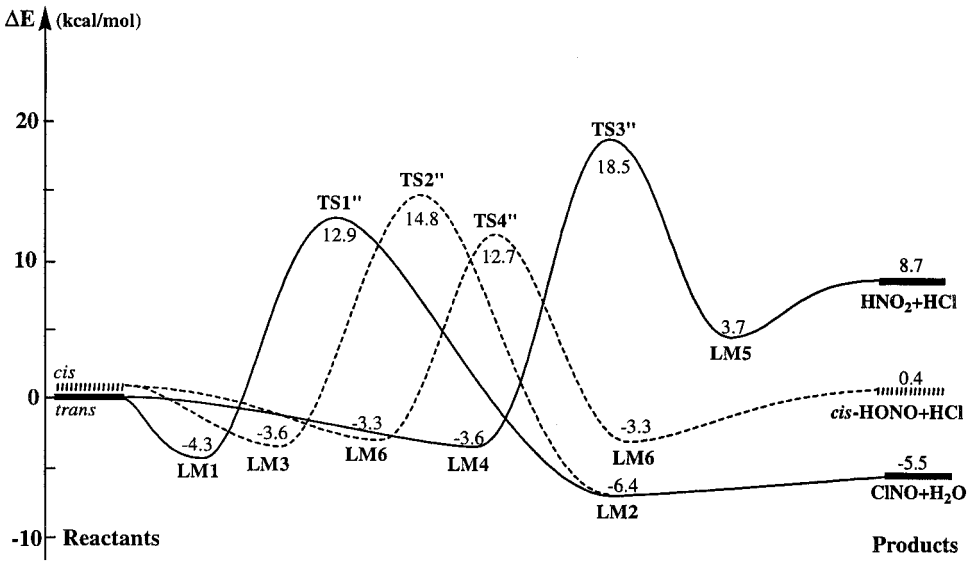

Figure 6. Energy diagram for the potential energy surface of the HONO + HCl reaction calculated in the framework of the G2M(RCC,MP2)// B3LYP/6-311G(d,p) approach. Solid lines connect the *trans*-HONO related channels, and the dotted lines connect the *cis*-HONO related channels.

TABLE 7: Molecular and Transition-State Parameters of the Reactants, Products, and Transition States of the HONO + HCl Reaction, Used for the TST Calculations of the Rate Constants[a]

species	I_i (amu)	frequencies (cm^{-1})
trans-HONO	see table 2	see table 2
cis-HONO	see table 2	see table 2
HCl	0.0, 5.8, 5.8	2927
TS1″	196.7, 558.8, 709.0	965*i*, 158, 186, 434, 470, 555, 661, 921, 1221, 1395, 2060, 3766
TS2″	178.9, 630.3, 769.7	988*i*, 121, 242, 404, 480, 520, 681, 948, 1207, 1337, 2012, 3731
TS3″	96.1, 713,5, 809.7	640*i*, 273, 355, 476, 916, 1030, 1126, 1290, 1478, 1700, 1987, 2219
TS4″	137.3, 559.4, 696.7	622*i*, 278, 364, 725, 815, 977, 1097, 1305, 1453, 1497, 1628, 1932
LM1	115.3, 1129.9, 1245.2	32, 43, 130, 394, 396, 545, 605, 783, 1268, 1823, 2782, 3773
LM2	305.8, 472.9, 740.4	110, 137, 169, 216, 294, 354, 445, 554, 1646, 2014, 3769, 3873
LM3	31.3, 1463.8, 1495.1	19, 46, 110, 350, 407, 575, 660, 851, 1305, 1759, 2811, 3609
LM4	139.2, 1071.2, 1210.4	15, 97, 106, 382, 416, 605, 652, 872, 1323, 1792, 2773, 3750
LM5	70.3, 1079.9, 1150.3	49, 104, 152, 414, 475, 805, 1076, 1402, 1545, 1676, 2722, 3153
LM6	135.4, 954.6, 1090.0	38, 87, 108, 280, 294, 662, 726, 928, 1346, 1691, 2850, 3559
HNO_2	16.7, 136.8, 153.5	800, 1069, 1408, 1542, 1678, 3145
ClNO	20.4, 335.3, 355.7	318, 591, 1968
H_2O	2.3, 4.1, 6.4	1639, 1809, 3906

[a] Calculated at the B3LYP/6-311G(d,p) level.

have been investigated by means of ab initio MO and transition-state theory calculations. For the HONO + NO_2 reaction, several possible reaction pathways have been identified, including O-transfer from NO_2 to HONO and H and HO abstraction from HONO by NO_2. Interestingly, the HO abstraction channel leading to the formation of HNO_3 and NO have been shown to be most favorable with the predicted barrier heights of about 32 kcal/mol for both cis and trans reactions. The calculated rate constant for the reaction at 300 K is on the order of 10^{-12} cm^3 mol^{-1} s^{-1}.

For the HONO + O_3 reaction, a barrier height of 15.0 kcal/mol has been predicted for the most favorable channel occurring via a transition state connecting the O_3 + *cis*-HONO reactants with the O_2 ($^1\Delta$) + HNO_3 products. TST calculations predict a rate constant of 5.7×10^{-2} cm^3 mol^{-1} s^{-1} for this channel at 300 K. The *trans*-HONO + O_3 reaction was also shown to take place via a cyclic transition state, leading directly to $HOOONO_2$ with a 23.9 kcal/mol barrier.

For the *trans*- and *cis*-HONO + HCl → H_2O + ClNO reactions, our G2M calculations predicted their barrier heights to be 12.9 and 14.4 kcal/mol, respectively. TST calculations gave the respective rate constants, 1.3×10^2 and 0.13×10^2 cm^3 mol^{-1} s^{-1} at 300 K, noticeably lower than the experimentally estimated upper limit, $\sim 1 \times 10^5$ cm^3 mol^{-1} s^{-1}.

On the basis of the aforementioned theoretical results, it can be concluded that the three homogeneous gas-phase reactions are probably unimportant in atmospheric chemistry; however, both NO_2 and HCl reactions may become significant under high temperature/pressure propellant combustion conditions.

The large deviation between the predicted and the estimated upper limit in each of the three reactions investigated deserves further comments. First of all, as alluded to earlier, the pronounced catalytic effects of the reactor surface on thermal reactions of highly polar molecules such as HONO[40] and HCOOH[41] are well-known. These deleterious effects make it impossible to extract their small homogeneous gas-phase contributions. For the HONO system, its source molecules, NO, NO_2, and H_2O, may also complicate the chemistry involved. Second, the predicted TS parameters, particularly energy barriers, may be too high by 2−3 kcal/mol, which is within the combined errors of the reactants and TS, ± 2 kcal/mol, at the G2M(RCC, MP2) level of theory.[26] These discrepancies could only be settled by a truly homogeneous experiment carried out in a shock tube, however.

Acknowledgment. This work was sponsored partially by Emory University and partially by the Caltech Multidisciplinary University Research Initiative under ONR Grant No. N00014-

95-1-1388, Program Manager, Dr. J. Goldwasser. One of us (X.L.) acknowledges a Visiting Fellowship from the Cherry L. Emerson Center for Scientific Computation.

References and Notes

(1) Kuo, K. K.; Summerfield, M. *Fundamentals of Solid Propellant Combustion, Progress in Astronautics and Aeronautics*; AIAA, Inc.: New York, 1984; Vol. 90.

(2) Alexander, M. H.; Dagdigian, P. J.; Jacox, M. E.; Kolb, C. E.; Melius, C. F.; et al. *Prog. Energy Combust. Sci.* **1991**, *17*, 263.

(3) Adams, G. F.; Shaw, R. W., Jr. *Annu. Rev. Phys. Chem.* **1992**, *43*, 311.

(4) Mebel, A. M.; Lin, M. C.; Morokuma, K.; Melius, C. F. *J. Phys. Chem.* **1995**, *99*, 6842.

(5) Cox, R. A. *J. Photochem.* **1971**, *3*, 175.

(6) Mielke, Z.; Tokhadze, K. G.; Latajka, Z.; Ratajczak, E. *J. Phys. Chem.* **1996**, *100*, 539.

(7) Mielke, Z.; Latajka, Z.; Kolodziej, J.; Tokhadze, K. G. *J. Phys. Chem.* **1996**, *100*, 11610.

(8) Wierzejewska, M.; Mielke, Z.; Wieczorek, R.; Latajka, Z. *Z. Chem. Phys.* **1998**, *228*, 17.

(9) Jursic, B. S. *Chem. Phys. Lett.* **1999**, *299*, 334.

(10) Wieczorek, R.; Latajka, Z.; Lundell, J. *J. Phys. Chem. A* **1999**, *103*, 6234.

(11) Mebel, A. M.; Lin, M. C.; Morokuma, K. *Int. J. Chem. Kinet.* **1998**, *30*, 729.

(12) Mebel, A. M.; Lin, M. C.; Melius, C. F. *J. Phys. Chem.* **1998**, *102*, 1803.

(13) Lu, X.; Musin, R. N.; Lin, M. C. *J. Phys. Chem. A* **2000**, *104*, 5144.

(14) Streit, G. E.; Wells, J. S.; Fehsenfeld, F. C.; Howard, C. J. *J. Chem. Phys.* **1979**, *70*, 3439.

(15) Kaiser, E. W.; Japar, S. M. *Chem. Phys. Lett.* **1977**, *52*, 121.

(16) Gertner, B. J.; Hynes, J. T. *Science* **1996**, *271*, 1563.

(17) Zhang R.; Len, M. T.; Keiser, L. F. *J. Phys. Chem.* **1996**, *100*, 339.

(18) Wingen, L. M.; Barney, W. S.; Lakin, M. J.; Brauers, T.; Finlayson-Pitts, B. J. *J. Phys. Chem.* A **2000**, *104*, 329.

(19) Becke, A. D. *J. Chem. Phys.* **1992**, *96*, 2155.

(20) Becke, A. D. *J. Chem. Phys.* **1992**, *97*, 9173.

(21) Becke, A. D. *J. Chem. Phys.* **1993**, *98*, 5648.

(22) Lee, C.; Yang, W.; Parr, R. G. *Phys. Rev.* **1988**, *B37*, 785.

(23) Hehre, W.; Radom, L.; Schleyer, P. v. R.; Pople, J. A. *Ab Initio Molecular Orbital Theory*; Wiley: New York, 1986.

(24) Gonzalez, C.; Schlegel, H. B. *J. Chem. Phys.* **1989**, *90*, 2154.

(25) Purvis, G. D.; Bartlett, R. J. *J. Chem. Phys.* **1982**, *76*, 1910. (b) Hampel, C.; Peterson, K. A.; Werner, H.-J. *Chem. Phys. Lett.* **1992**, *190*, 1. (c) Knowles, P. J.; Hampel, C.; Werner, H.-J. *J. Chem. Phys.* **1994**, *99*, 5219. (d) Deegan, M. J. O.; Knowles, P. J. *Chem. Phys. Lett.* **1994**, *227*, 321.

(26) Mebel, A. M.; Morokuma, K.; Lin, M. C. *J. Chem. Phys.* **1995**, *103*, 7414.

(27) Curtiss, L. A.; Raghavachari, K.; Trucks, G. W.; Pople, J. A. *J. Chem. Phys.* **1991**, *94*, 7221.

(28) Pople, J. A.; Head-Gordan, M.; Raghavachari, K. *J. Chem. Phys.* **1987**, *87*, 5768.

(29) Frisch, M. J.; Trucks, G. W.; Schlegel, H. B.; Gill, P. M. W.; Johnson, B. G.; Robb, M. A.; Cheeseman, J. R.; Keith, T.; Petersson, G. A.; Montgomery, J. A.; Raghavachari, K.; Al-Laham, M. A.; Zakrzewski, V. G.; Ortiz, J. V.; Foresman, J. B.; Cioslowski, J.; Stefanov, B. B.; Nanayakkara, A.; Challacombe, M.; Peng, C. Y.; Ayala, P. Y.; Chen, W.; Wong, M. W.; Andres, J. L.; Replogle, E. S.; Gomperts, R.; Martin, R. L.; Fox, D. J.; Binkley, J. S.; Defrees, D. J.; Baker, J.; Stewart, J. P.; Head-Gordon, M.; Gonzalez, C.; Pople, J. A. *Gaussian 94*, revision D.3; Gaussian, Inc.: Pittsburgh, PA, 1995.

(30) MOLPRO is a package of ab initio programs written by H.-J. Werner and P. J. Knowles, with contributions from J. Almlöf, R. D. Amos, M. J. O. Deegan, S. T. Elbert, C. Hampel, W. Meyer, K. Peterson, R. Pitzer, A. J. Stone, P. R. Taylor, and R. Lindh.

(31) Chase, M. W., Jr. NIST-JANAF Thermochemical Tables, 4th ed.; *J. Phys. Chem. Ref. Data*, 1998.

(32) McGrath, M. P.; Francl, M. M.; Rowland, M. S.; Hehre, M. J. *J. Phys. Chem.* **1988**, *92*, 5352.

(33) Sumath, R.; Peyerimhoff, S. D. *J. Chem. Phys.* **1997**, *107*, 1872.

(34) Jursic, B. S.; Klasinc, L.; Pecur, S.; Pryor, W. A. *Nitric Oxide* **1997**, *1*, 494.

(35) Huber, K. P., Herzberg, G. *Molecular Spectra and Molecular Structure, IV. Constants of Diatomic Molecules*; Van Nostrand Reinhold Co.: New York, 1979.

(36) Li, Y.; Iwata, S. *Bull. Chem. Soc. Jpn.* **1997**, *70*, 79.

(37) Hallou, A.; Schriver-Mazzuoli, L.; Schriver, A.; Sanna, N.; Pieretti, A. *Asian J. Spectros.* **1997**, *1*, 189.

(38) Pieretti, A.; Sanna, N.; Hallou, A.; Schriver-Mazzuoli, L.; Schriver, A. *J. Mol. Struct.* **1998**, *447*, 223.

(39) Steinfeld, J. I.; Francisco, J. S.; Hase, W. L. *Chemical Kinetics and Dynamics*; Prentice Hall: Englewood Cliffs, NJ, 1989.

(40) Kaiser, E. W.; Wu, C. H. *J. Phys. Chem.* **1977**, *81*, 1701.

(41) Stein, S. E.; Benson, S. W.; Golden, D. M. *J. Catal.* **1976**, *44*, 429.